The validity of the non-linear shell model for localized dipole moments in $Li_xK_{1-x}TaO_3$

1991 J. Phys.: Condens. Matter 3 3689

(http://iopscience.iop.org/0953-8984/3/21/002)

J. Phys.: Condens. Matter 3 (1991) 3689–3695. Printed in the UK

The validity of the non-linear shell model for localized dipole moments in $Li_xK_{1-x}TaO_3$

M G Stachiotti†, R L Migoni† and U T Höchli‡

† Instituto de Fisica, Universidad Nacional de Rosario, 27 de Febrero 210 Bis, 2000 Rosario, Argentina

‡ IBM Research Division, Zurich Research Laboratory, CH-8803 Rüschlikon, Switzerland

Received 24 January 1991

Abstract. The temperature dependence of the off-centre Li position and surrounding lattice polarization in Li:$KTaO_3$ is calculated within the quasiharmonic approximation using a non-linear polarizability model. The Li displacement is found to be almost independent of temperature. Both the total dipole moment of the region where the Li dipole moment is reinforced by the lattice polarization and the size of this region become smaller with decreasing temperature. The Li displacement as well as the total dipole moment are described quantitatively by this model, provided that the Li concentration is below ~1%.

1. Introduction

The perovskite crystals have one of the most extensively investigated structures [1]. It is remarkable that for pure $KTaO_3$ as well as for mixed KTN crystals, transitions to ordered polar phrases have been predicted correctly on the basis of a non-linear polarizability model [2]. It is, however, well established that disordered phenomena are also present in the mixed KTN phases [3] and in particular in $KTaO_3$:Li where evidence for disorder is overwhelming [4].

It is thought that the the dipole moments associated with off-centre Li impurities interact in a random way and give rise to a dipole glass configuration analogous to a spin glass [4, 5]. It should then be possible, by applying the non-linear polarizability model, to compute the single-spin properties and ultimately the relevant parameters of the interaction distribution between Li dipoles. This interaction distribution is still somewhat controversial and determines the character of the polar phase, whether ordered or disordered.

The single-ion properties of Li constitute the basis of such an investigation. We wish thus to apply the non-linear polarizability model to this defect and establish its model properties at all temperatures. Next we shall compare the predictions with experimental evidence to show that single-ion properties are well described by theory but that there is an extremely narrow experimental range of Li concentration where single-ion properties are relevant. Based on the success of the model we shall try to develop some aspects of the interaction between Li ions in this range.

0953-8984/91/203689 + 07 $03.50

2. Theory

The Li^+ ion, when replacing K^+ in $KTaO_3$, goes to one of the six off-centre positions along the [001] cubic directions [6]. The resulting dipole moment polarizes the lattice such that a region appears around the Li whose total dipole moment P_{loc} is larger than the one corresponding to the Li displacement P_{Li}. This fact is supported by experimental evidence [7] as well as a model calculation [8]. For Li concentrations below 4% the system undergoes a transition to a dipole glass phase, while at higher concentrations a mixed ferroelectric behaviour appears [9]. In order to understand the origin of the glassy behaviour it is interesting to investigate the size and shape of the polarized region as a function of temperature. There are two points of view with regard to this phenomenon. According to Vugmeister *et al* [10] $P_{loc} = (\varepsilon\gamma/3)P_{Li}$ where $\varepsilon(T)$ is the susceptibility of pure $KTaO_3$ and γ is a coupling constant. P_{loc} should thus increase with decreasing T. It has also been argued, however, that the total dipole moment is proportional to the correlation volume, which is also only weakly temperature dependent [11].

In this paper we study the temperature dependence of the lattice configuration around a Li defect in the framework in the non-linear shell model previously used to determine the static configuration of the system [8]. The defect lattice equilibrium condition in the absence of external force is

$$\partial F(s, T)/\partial s = 0 \tag{1}$$

where $F(s, T)$ is the Helmholtz free energy and s are the thermal mean displacements in the defect lattice with respect to the perfect lattice positions. $F(s, T)$ can be evaluated in a quasiharmonic approximation as

$$F^{qh}(s, T) = \Phi(s) + F_s(s, T) \tag{2}$$

where Φ is the total potential energy of the lattice, including the interaction with the defect. F_s is the harmonic free energy of vibrations around the thermal mean positions:

$$F_s = -1/\beta \ln \mathrm{Tr} \exp(-\beta H_s) \tag{3}$$

with

$$H_s = E_k + \tfrac{1}{2}\Phi_{ij}^{(2)}(s)\xi_i\xi_j \tag{4}$$

where $\Phi_{ij}^{(n)}(s)$ are the n^{th} derivatives of Φ evaluated at the mean positions and ξ denote the dynamic displacements from these positions. By replacing (4) in the previous equations the equilibrium condition gives

$$\Phi_i^{(1)}(s) + \tfrac{1}{2}\Phi_{ijk}^{(3)}(s)\langle\xi_j\xi_k\rangle = 0 \tag{5}$$

where the angle brackets denote thermal averages. It is well known that for the equilibrium condition the quasiharmonic approximation is equivalent to the lowest order of perturbation theory for the free energy, which corresponds to retaining only those terms proportional to $[\Phi^{(3)}]^2$ and $\Phi^{(4)}$ [12].

Setting $\Phi = \varphi + V$, where φ is the host lattice potential and V describes the defect–lattice interaction, we neglect the contribution of the latter to the second term in (5). By developing $\varphi^{(n)}(s)$ around the perfect lattice position $s = 0$ we obtain from (5).

$$\varphi_i^{(1)} + \varphi_{ij}^{(2)}s_j + \tfrac{1}{2}\varphi_{ijk}^{(3)}s_js_k + \ldots + \tfrac{1}{2}(\varphi_{ijk}^{(3)} + \varphi_{ijkl}^{(4)}s_l + \ldots)\langle\xi_j\xi_k\rangle = f_i(s) \tag{6}$$

where $f_i(s) = -V_i^{(1)}(s)$ is the defect force. Since the perfect lattice positions correspond

to the minimum of φ, we have $\varphi_i^{(1)} = 0$. Moreover, as we will see below, we have $\varphi_{ijk}^{(3)} = 0$ for our model. The averages $\langle \xi_i \xi_k \rangle$ refer to the defect lattice and can be developed around $s = 0$ as follows:

$$\langle \xi_i \xi_j \rangle = \langle \xi_i \xi_j \rangle_0 + \partial \langle \xi_i \xi_j \rangle / \partial s_k |_{s=0} s_k + \ldots . \tag{7}$$

The second term vanishes because $\varphi^{(3)} = 0$ in the present case. Due to the definition of the s as displacements from the perfect lattice positions, they include a term of zero order in $\varphi^{(4)}$. Therefore the first term of (7) gives a contribution of the $\varphi^{(4)}$ order to (6) and the contribution of the next non-vanishing term is of the $[\varphi^{(4)}]^2$ order, which will be neglected. With all these considerations (6) becomes:

$$(\varphi_{ij}^{(2)} + \tfrac{1}{2} \varphi_{ijkl}^{(4)} \langle \xi_l \xi_j \rangle_0) s_j + 1/3!\, \varphi_{ijkl}^{(4)} s_j s_k s_i = f_i(s). \tag{8}$$

For these calculations we use a shell model where every ion is polarizable and the oxygen ion in particular includes a fourth-order core–shell coupling in the direction of its neighbouring Ta^{5+} ion. Short-range forces couple each oxygen shell to those of its nearest K^+, Ta^{5+} and O^{2-} ions. More details of this model are given in [13]. From the model potential we obtain an equation analogous to (8) for the thermal mean displacements of their cores (u) and shells (w):

$$f^{\mathrm{T}} = (\mathbf{S} + \mathbf{C}^{zz})u + (\mathbf{S} + \mathbf{C}^{zy})w \tag{9}$$

$$f^{s} = (\mathbf{S} + \mathbf{C}^{yz})u + [\mathbf{S} + \mathbf{C}^{yy} + \mathbf{K}(\mathbf{T})]w + 1/3!\, K_{\mathrm{OB,B}} \mathbf{L}{:}w{\otimes}w{\otimes}w \tag{10}$$

where the subscripts O and B denote the oxygen ion and the B site of the perovskite lattice, respectively, and f^{T} is the total force exerted by the defect on the lattice ions and f^{s} is the corresponding force on the shells. We consider the same defect–lattice interaction as used previously [8]. **S** is the short-range force constant matrix and the **C** matrices represent the Coulomb interaction, z denoting ionic changes and y shell charges. The matrix **L** picks up the components of w appropriate to the non-linear anisotropic interaction described above. The matrix **K(T)** is diagonal and contains the harmonic core–shell coupling constants with the only modification, for the case of the oxygens, as follows:

$$\mathbf{K}_{\alpha}^{\mathrm{O}} \alpha(\mathbf{T}) = \mathbf{K}_{\mathrm{OB}} + \tfrac{1}{2} \mathbf{K}_{\mathrm{OB,B}} \langle \xi_{\alpha}^2(\mathrm{O}_{\alpha}) \rangle_0 \tag{11}$$

where $\xi(\mathrm{O})_{\alpha}$ is the dynamic shell displacement for an oxygen whose neighbouring Ta is in the α direction. The thermal average in (11) is obtained self-consistently in the pure lattice. It is this renormalization that gives rise to a temperature dependence of the model parameters.

Equations (9) and (10), together with the equilibrium condition for the defect, are solved as explained in [8]. We performed calculations at 300 K, 100 K and 25 K with the results shown in figure 1, which is a schematic representation of the polarized lattice region reinforcing the defect dipole moment, shown in detail in figure 4 of [8]. Each box represents a unit cell, the arrows denote the defect dipole moments included in the corresponding box and the values indicate the total dipole moment of the corresponding unit cell. We note that the Li displacement is almost independent of temperature. The total effective dipole moment remains fairly constant above 100 K, while it *decreases* significantly at 25 K. Similar behaviour is observed for the size of the polarized region, thus suggesting that the two magnitudes are closely related. These temperature effects differ from those predicted by Vugmeister *et al* [10], whose theory takes into account

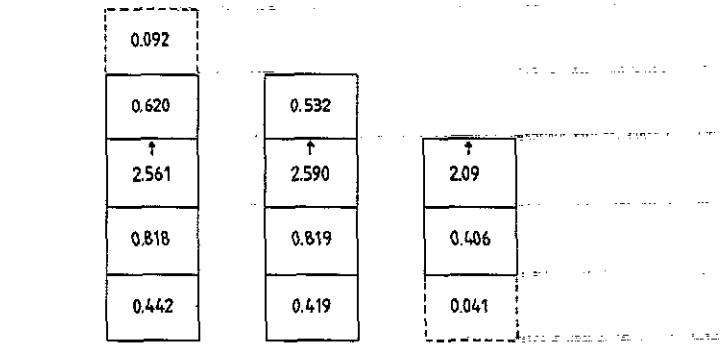

Figure 1. Schematic representation of the polarized region reinforcing the Li dipole at different temperatures. Each box corresponds to the height of a lattice constant $a = 4$ Å and the values inserted give its dipole moment in units of P_{Li}. The position of the Li dipole is indicated by the arrow.

the electrostatic interaction of a given dipole with the field originated by other defects and modified by lattice phonons [14]. Moreover, they treat an effective diatomic cubic lattice with a Lorentz factor γ for the defect site defined for the perovskite cell as follows [15]:

$$\gamma_K = \frac{P_z\,(\mathrm{Ta}) + P_z\,(\mathrm{K}) + (1-3\alpha)P_z\,(\mathrm{O}_z) + (2+3\alpha)P_z\,(\mathrm{O}_x)}{P_z\,(\mathrm{Ta}) + P_z\,(\mathrm{K}) + P_z\,(\mathrm{O}_z) + 2P_z\,(\mathrm{O}_x)} \tag{12}$$

with $\alpha = 0.69$. Therefore this theory does not allow a self-consistent evaluation of γ. Nor is it clear whether such a factor can be defined uniquely in an inhomogeneously polarized lattice.

Attempts to calculate P_{Li} and P_{loc} on the basis of a linearly polarizable [16] point charge model yield $P_{Li} = 1.1e$ Å and $P_{loc} \sim 1e$ Å, independently of T. The predictions of the non-linear shell model [2] are thus quite distinct from earlier predictions based on interaction between impurity dipoles and soft modes [10, 14] and based on linear polarizability [3]. The finding may thus be subjected to experimental test.

3. Summary of the experimental evidence and interpretation

We start by summarizing the experimental evidence for our theoretical results. The Li displacement δ was obtained from a measurement of the energy spectrum of the ^{7}Li nuclear dipole in a magnetic field. This experiment determined the average electric field gradient at the Li position during the nuclear coherence period, about 10^{-5} s. The determination of the displacement δ is based on a model calculation: the surrounding ions are considered to be nominal ionic charges giving rise to a field gradient at the Li site that depends on position. Within this approximation, the displacement was found [17] to be 1.26 Å. This displacement corresponds to the maximum distortion possible if both Li and the ligands are considered hard spheres with nominal ionic radii. According to the experiment, δ is independent of T and of Li concentration at low x.

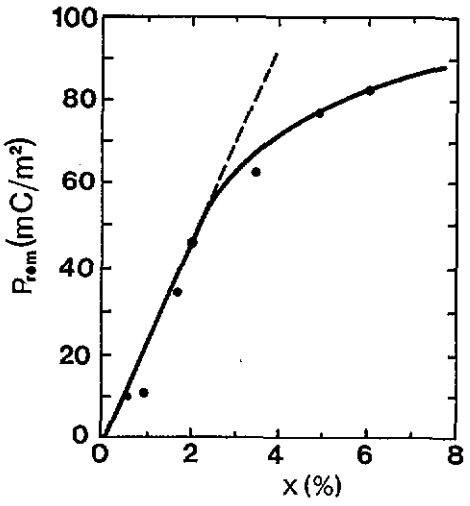

Figure 2. Polarization at T_f for samples with different Li concentrations x. The tangent corresponds to $\partial P/\partial x = 1.1\ \mathrm{C\,m^{-2}}$. Theory predicts $\approx 2\ \mathrm{C\,m^{-2}}$ and a saturation at $50\ \mathrm{mC\,m^{-2}}$. Data are from [7].

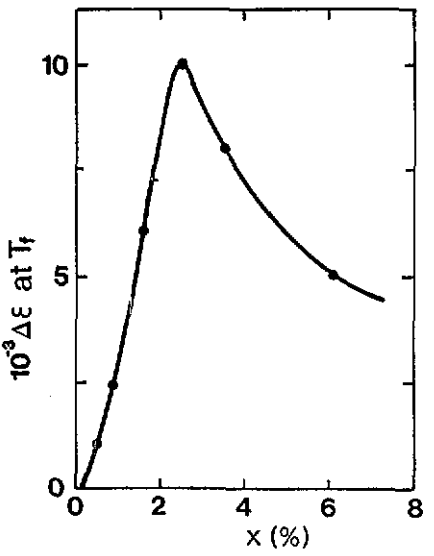

Figure 3. Dielectric susceptibility versus Li concentration x at T_f. For low x, evaluation of cluster size (equation (13)) is possible.

The local polarization around one displaced Li exceeds that of the bare Li: an experiment in which the KTL was cooled in a field and where the charge release was measured on reheating gave a local polarization of about $4.5e$ Å per Li site. The effective temperature for freezing the polarization can be estimated to be about 25 K in this experiment. Upon further cooling the local polarization is frozen in at the value obtained with $T_f = 25$ K. Since P_{loc} is not necessarily at equilibrium below T_f, its temperature dependence below T_f is irrelevant for the evaluation of this model. We find thus that the value for P_{Li} is correctly predicted by both the non-linear and the linear polarizability models. The enhancement factor $P_{loc}/P_{Li} \simeq 4$ is correctly predicted by the non-linear polarizability theory. The linear polarizability has, of course, a screening effect, thus the enhancement factor predicted [16] is <1. The phonon coupling model [10] overestimates $P_{loc}/P_{Li} \sim \varepsilon\gamma/3 \sim 10^2$ by a factor of 25.

The spatial extension of the local polarization can be obtained from figure 1: 99% of the polarization is found in a region whose radius r is about three lattice constants. Accordingly, the total polarization should be a linear function of Li concentration for $x < (r/a)^{-3} \simeq 0.04$ with a slope $\partial P/\partial x = NP_{loc} = 1.1\ \mathrm{C\,m^{-2}}$. Furthermore P should saturate for large x at a value of $50\ \mathrm{mC\,m^{-1}}$. Inspection of figure 2 confirms these results almost quantitatively. Deviations and the rounding at about $x = 0.04$ are attributed to interaction between local polarizations which increase as the concentration increases.

Above T_f, P_{loc} is a dynamic variable to be measured by susceptibility. Independent local polarizations have a Debye susceptibility ε_d given by $\varepsilon_d \sim NP_{loc}^2/3kT\varepsilon_0$ which is clearly contrary to observation [9]. Instead ε rises faster than with $1/T$, and below the freezing temperature it stays about constant. In figure 3 we have plotted $\varepsilon(x)$ at T_f for various concentrations. We note a large x-dependent enhancement for which we have

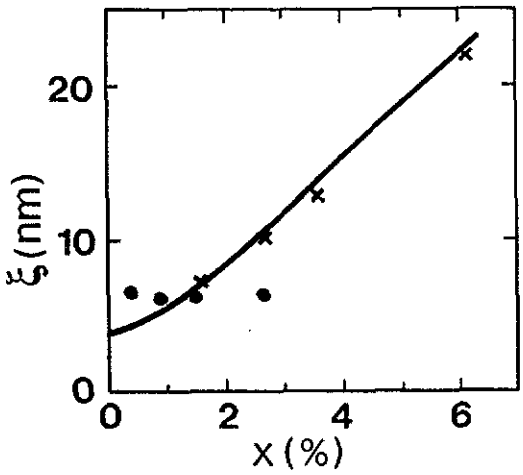

Figure. 4. Polarization correlation length (or cluster site) (×) from second-harmonic generation and cluster size from dielectric susceptibility (○).

a plausible argument. Assume that the effect of interaction is to align dipoles within a short region and that these regions are mutually independent. In this (independent-cluster) approximation

$$\varepsilon \sim (N/n)\,(nP_{\mathrm{loc}})^2/3kT\varepsilon_0 \sim n\varepsilon_{\mathrm{D}}. \tag{13}$$

We evaluate the correlation factor n from the experiment and express it in terms of length ξ

$$\xi = a(n/x)^{1/3}. \tag{14}$$

In figure 4 this length is plotted versus x and is found to be $\simeq 6$ nm for $x < 0.02$. As x grows larger, this approximation is bound to fail. A direct observation of polar correlation is, however, possible in this regime by means of second-harmonic light generation [18], the results of which are also plotted in figure 4. We note that the two data sets are compatible and that both present clear evidence for correlation which is a direct consequence of interaction between the local polarizations.

We note that within the independent-cluster approximation, the correlation length is of no consequence for the total polarization: the polarization per cluster increases at the same rate as the number of clusters decreases. Our findings are thus internally consistent and consistent with cluster formation. The number of local polarizations forming a cluster is, however, an ingredient that is not taken into account by present theory but a plausible extension based on interaction between local polarizations is likely to do so.

4. Conclusion

The non-linear shell model accounts for the local properties in a quantitative way: it predicts the value of the Li displacement in $KTaO_3$ and the enhancement of the local polarization due to the polarization cloud forming around Li both as a function of

temperature. It also predicts that the spatial extension of the polarization cloud is of the order of 25 unit cells which allows the qualitative conclusion that Li concentrations above 1% should give rise to interaction between local polarizations. All of these features are borne out by experiment. Our microscopic model includes the short-range interactions between the Li^+ and the surrounding ions, which are essential to explain the appearance of a lattice region reinforcing the Li dipole moment.

References

[1] Lines M E and Glass A M 1977 *Principles and Application of Ferroelectrics, and Related Materials* (Oxford: Clarendon p 138
[2] Migoni R L, Bilz H and Bäuerle D 1976 *Phys. Rev. Lett.* **37** 1155
[3] van der Klink J J, Rod S and Châtelain A 1986 *Phys. Rev.* B **33** 2084
[4] Höchli U T and Knorr K 1991 *Adv. Phys.* **39** 405
[5] Binder K and Young A P 1986 *Rev. Mod. Phys.* **58** 801
[6] van der Klink J J, Rytz D, Borsa F and Höchli U 1983 *Phys. Rev.* B **27** 89
[7] Höchli U, Weibel H and Boatner L 1979 *J. Phys. C: Solid State Phys.* **12** L563
[8] Stachiotti M and Migoni R 1990 *J. Phys.: Condens. Matter* **2** 4341
[9] Höchli U and Maglione M 1989 *J. Phys.: Condens. Matter* **1** 2241
[10] Vugmeister B, Glinchuk M and Pechenyi A 1984 *Sov. Phys.–Solid State* **26** 2036
[11] Höchli U and Baeriswyl D 1984 *J. Phys. C: Solid State Phys.* **17** 311
[12] Fischer K 1959 *Z. Phys.* **155** 59
[13] Perry C, Currat R, Buhay H, Migoni R, Stirling W and Axe J 1989 *Phys. Rev.* B **39** 8666
[14] Vugmeister B and Glinchuk M 1980 *Sov. Phys.–JETP* **52** 482; 1983 *Solid State Commun.* **48** 503
[15] Vugmeister B and Glinchuk M 1990 *Rev. Mod. Phys.* **62** 993
[16] van der Klink J J and Khanna S N 1984 *Phys. Rev.* B **29** 2415
[17] van der Klink J J and Borsa F 1984 *Phys. Rev.* B **30** 52
[18] Azzini G A, Banfi G P, Giulott E and Höchli U T 1991 *Phys. Rev.* B at press
Höchli U T, Knorr K and Loidl A 1990 *Adv. Phys.* **39** 405